This full text paper was peer-reviewed at the direction of IEEE Instrumentation and Measurement Society prior to the acceptance and publication.

Intra-Operative 3D Registration of MIS Reconstructed Surfaces to Pre-Operative Models*

Georgia Peleka, Georgios Zampokas, Ioannis Mariolis, Sotiris Malasiotis, Dimitrios Tzovaras
Information Technologies Institute
Centre for Research & Technology - Hellas
Thessaloniki, Greece
{gepe, gzampokas, ymariolis, malasiot, tzovaras}@iti.gr

***Abstract*—This work focuses on the challenges of 3D surface registration in MIS applications. A novel dataset has been created based on CT scans of a knee phantom and pre-operative 3D models of the meniscus are extracted. Four state-of-the-art 3D registration methods are evaluated on the registration of noisy patches segmented from the models' surface to the model itself in an attempt to objectively compare their performance using ground-truth correspondences. The results of this analysis provide useful insight on the problem at hand and indicate where our focus should be steered in order to successfully tackle it.**

***Index Terms*—surface registration, Minimally Invasive Surgery, pre-operative models**

I. Introduction

There are many existing research works trying to apply *Augmented Reality* (AR) in *Minimal Invasive Surgery* (MIS) to help overcome some of the current limitations. The general call is for on-the-fly fusion between other modalities of the MIS system and the MIS video, creating a composite view that conveys additional information (such as the location of important subsurface structures). In this work, we are performing a comparative study between different approaches for 3D surface registration of intra-operative MIS data to pre-operative 3D models of the anatomical structures of interest. For this purpose, a knee phantom has been employed and a novel dataset has been created including 3D models of the meniscus, as well as noisy segments of the models' surface. This approach allows for the knowledge of ground-truth correspondences between the models and the 3D surface segments facilitating the proposed evaluation procedure. Valuable conclusions are derived on the usefulness of the examined methods and on future directions that should be further investigated.

Previous works on MIS data registration can be broadly divided into two categories, those that tackle the problem with a semi-automatic approach and those that use a more constraint and automatic one. In works where a semi-automatic approach is adopted, either the surgeon roughly aligns the 3D model to the camera view as an initialization step, or on-tissue artificial markers are being utilized for assisting the registration process.

Simpfendrfer et al. [1] propose a marker-assisted 2D-3D point correspondence registration of *Transrectal Ultrasonography* (TRUS) data to real-time video feed. Custom-developed needles with colored heads that are placed into the prostate surface as soon as the organ is exposed play the role of markers. These navigation aids are segmented in three-dimensional (3D) TRUS data that is acquired right after their placement and then are continuously acquired by the surgical navigation system. The markers are tracked in real time and the registration between TRUS image and laparoscopic video is computed through two dimensional to three dimensional (2D-3D) point correspondences.

*The research leading to these results has received funding from the European Communitys Framework Programme Horizon 2020 under grant agreement No 732515 SMARTsurg.

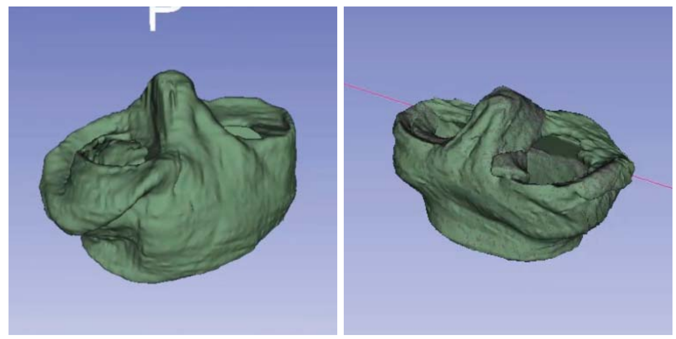

Fig. 1: Healthy (*left*) and torn (*right*) meniscus 3D models, extracted through manual annotation in 3D Slicer software.

Figl et al. [2] constructed a 4D motion model of the heart and achieved registration in two phases; first, the temporal alignment is achieved and then the spatial alignment follows. Spatial alignment is done manually by the surgeon at the beginning of the procedure, and the correspondence points are computed based on photo-consistency. Having established temporal registration from the first phase, the remaining motion is considered to be rigid apart from possible deformation of the heart due to breathing function. The main parameters for the 4D motion model, heart rate, and respiratory frequency were determined through image processing. By comparing one of the images of the beating heart within a video sequence with all the others they were able to determine the parameters using cross-correlation as a similarity measure. The frequencies were then found as peaks in the Fourier transform of this function.

Li-Ming et al. [3] present a modified ICP registration method based on selected on model 3D reference positions. In the initialization step, an operator selected the surface points to be traced. Since the 3D surface reconstructed from the stereo video provided only a partial view of the kidney; the

978-1-5386-6628-9/18/$31.00 ©2018 IEEE

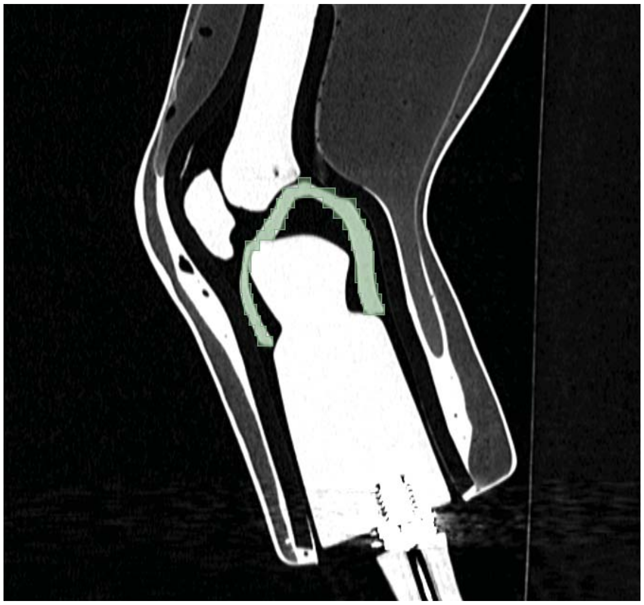

Fig. 2: Example annotation (green area) of meniscus anatomical region in 3D Slicer software.

ICP variant approach used firstly estimated the visibility of the preoperative 3D model in the current view before each iteration to restrict the point correspondence search only to the visible area of the organ.

Apart from the semi-automatic methods already described. there have been many works that adopted an automatic approach. W. Zeng et al. [4] presented the first method of large deformation surface 3D registration by solving Beltrami equations based on describing deformations with quasiconformal mappings. Their proposed approach is general, globally optimal, and robust. It can search for the desired registration in the complete space of diffeomorphisms, such as rigid motions, isometric transformations or conformal mappings. The global optimum is determined by the method uniquely up to a 3-dimensional transformation group, it can handle large surfaces with complicated topologies.

Pessaux et al. [5] suggested the use of fluorescence videography instead of a model for real-time video feed registration. They proposed the fluorescence-based enhanced reality (FLER) in which they present the fusion of fluorescence videography with AR to guide the intestinal resection and assess the vascular supply at the future anastomotic site.

Oktay et al. [6] proposed the computation and use of an insufflation model for their diffeomorphic non-rigid registration, which is a dense matching method driven by the gradient of local cross-correlation similarity measure. As a first step the deformations and organ shifts caused by gas pressure as computed, using a biomechanical model, which is based on the mechanical parameters and pressure level. This model is used to achieve an initial alignment with intra-operative images. This initial registration step accounts for both non-rigid and rigid transformations caused by the insufflation. The applied model couples the parameters with an intensity similarity measure and the finite element method (FEM) registration methods. At the next step, the diffeomorphic registration takes places, which has a higher degree of freedom refines the surface differences between the pre-operative image, warped according to the biomechanical model, and the intra-operative image.

II. Methods

We have researched and applied several automatic surface registration methods, as described in the next sections, spanning from simple rigid registration to more complex techniques where the deformations of the tissue is taken into account.

A. Point vs surface based registration, and Iterative Closest Point

As a first attempt traditional ICP algorithms for rigid registration where tested. Two approaches where researched. A point based one [7], where the 3D model and the 3D reconstructed image from the stereoscopic laparoscopic camera are treated as point clouds with no surface information. Thus, the registration is treated as a minimization problem, where the *Root Mean Squared (RMS)* distance between corresponding points once aligned has to be minimized.

The second attempt is a variant of ICP [8] where a set of initial rotation and translation states is used to avoid the main problem of the ICP algorithm, convergence in local minima. While the ICP may produce very good registration results with registration $error < 2mm$, the time need for registration is increased dramatically when the number of points increases, thus making it prohibitive for on-the-fly registration. An additional disadvantage of such techniques is that they do not take into account the deformations of the organ surface due to organ movement or by its interaction with the surgical instruments. Finally, the basic ICP algorithm does not produce optimal registration results when the target 3D scene is occluded (by other tissues or surgical instruments).

B. Optimal Step Non-rigid ICP Algorithm for Surface Registration

Trying to overcome the aforementioned constraints of the traditional ICP method, an extension of the ICP framework to non-rigid registration was also tested [9]. While retaining the convergence properties of the original ICP algorithm the optimal step non-rigid ICP framework allows the use of different regularizations.

The algorithm takes into account various stiffness weights and respectively deforms the template surface towards the target one. With this approach, the whole range of global and local deformations is recovered. For each stiffness weight, the optimal iterative closest point steps are being used to achieve the optimal corresponding deformation. For every step at first, a nearest-point search is being applied in order to estimate the preliminary correspondences. Then the optimal deformation of the template is calculated taking into account the fixed correspondences computed at the first step as well as the active stiffness weight. This procedure continues iteratively

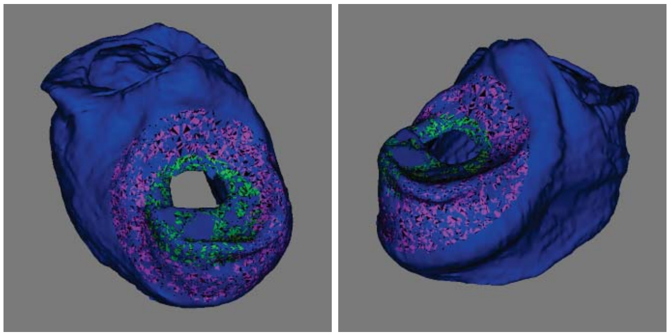

Fig. 3: Automatic segmentation of 3D model for *ground truth* extraction. The 3D pre-operative model (*blue*) is segmented in smaller regions (*magenta, green*) to simulate occlusions at the in-operative view.

with new correspondences found by searching from the displaced template vertices. Locally affine regularization is being applied, by assigning an affine transformation to each vertex and minimizing the difference in the transformation for the neighboring vertices.

It is shown that by using this regularization method the optimal deformation for the fixed correspondences and a fixed stiffness can be accurately determined with efficiency. The method achieves very good registration results for a wide range of initial conditions, whereas it is handling missing data robustly.

C. Coherent Point Drift point set registration

A related problem to surface-based registration is point set registration. These two different approaches are used interchangeably in the literature. Rigorously speaking, surface-based registration deals with surfaces that have connectivity information. On the other hand, point set based registration deals with sets of points without any connectivity information. The *Coherent Point Drift* (CPD) algorithm [10], is a probabilistic method utilized for both rigid and non-rigid point set registration.

The registration problem is being formulated as a probability density estimation problem, where one point set is represented using a *Gaussian Mixture Model (GMM)* and the other point set is considered as a set of observations generated according to the aforementioned GMM. The GMM centroids (representing the first point set) are being fitted to the data (the second point set) by maximizing the likelihood. The GMM centroids are being forced to move as a group coherently in order the topological structure of the point sets to be preserved. In the rigid case, a closed form solution derived from the maximization step of the EM algorithm [11] is used for optimization of the likelihood function, where the parameters of the GMM centroid locations are being re-configured so the coherence constrained can be imposed.

On the other hand, in the non-rigid case, the coherence constraint is imposed by regularizing the displacement field and using the variational calculus to derive the optimal transformation. The CPD algorithm can perform with great accuracy for both rigid and non-rigid transformations and can cope with the presence of noise, outliers and missing points.

D. Diffeomorphic non-rigid registration of shapes

Diffeomorphisms are broadly used in non-rigid methods for registration where large deformations are expected. Usually, the methodology refers to point-set registration methods, but in [12] authors have shown that diffeomorphisms can be used to registered 3D shapes also by utilizing a point-set representation for shapes since statistical shape analysis in this space is relatively straightforward. A joint clustering and diffeomorphism estimation strategy was introduced, allowing the simultaneous estimation of the correspondence and the fitting of a diffeomorphism between two point-sets.

Basically, within the proposed strategy the centres of the corresponding clusters for each point-set are always consistent since they are sharing the same index. In the course of clustering, the cluster center counterparts in each point-set are linked by a diffeomorphism and as a consequence are forced to move in lock-step with one another.

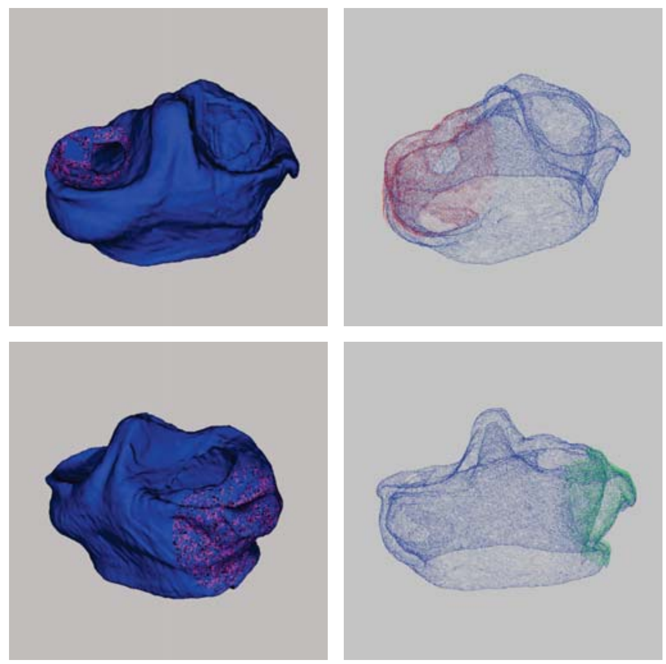

Fig. 4: Examples of segmentations from the constructed *ground truth* dataset. For every segmented region a mesh (*first column*) and a point-set representation (*second column*) are extracted.

III. Methods Evaluation

A. Ground truth dataset of meniscus phantom

In order to evaluate the aforementioned methods, an automatic segmentation framework was developed in the scope of this work. The 3DSlicer software [13], was used to review pre-operative CT images of a knee phantom in order to extract the 3D model of the anatomical structure of meniscus. We had different meniscus models scanned within the knee phantom

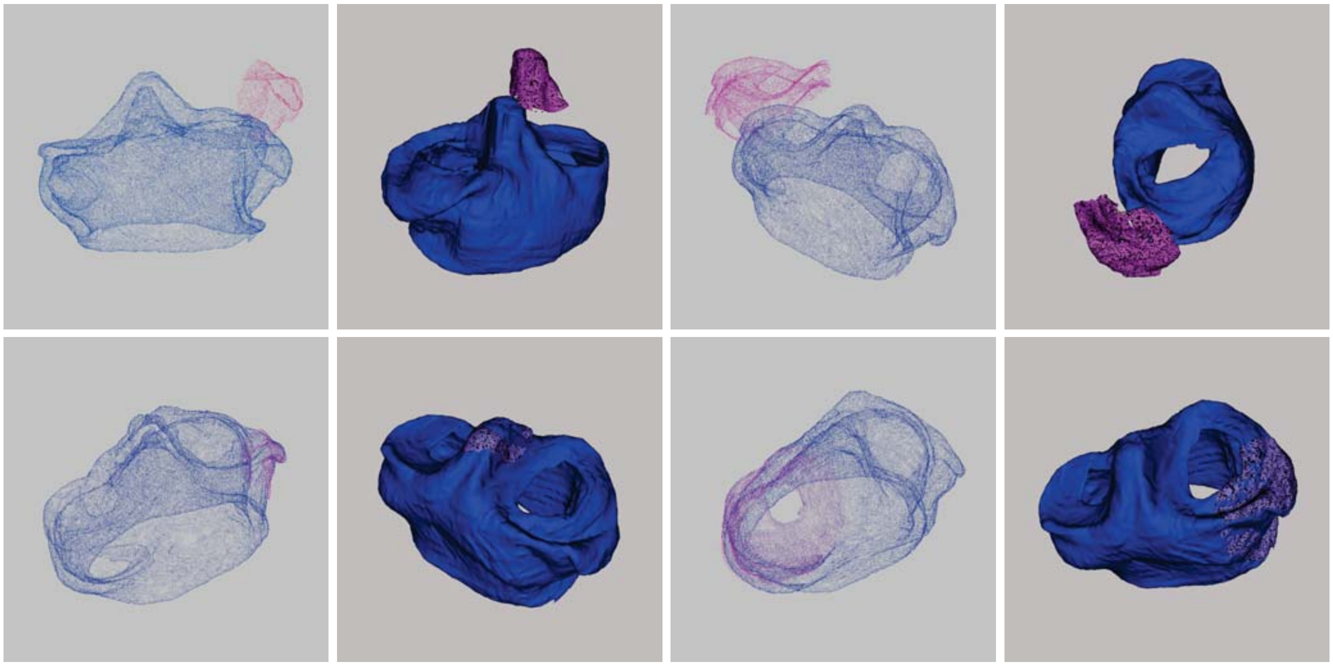

Fig. 5: Examples of good registration results. The initial positions of the template with respect to the target are shown on the top row. The corresponding successful registration results with $RMSerror < 10^{-3}mm$ are shown on the bottom row (from left to right: ICP, optimal step non-rigid ICP, CPD, diffeomorphic non-rigid).

corresponding to various meniscus lacerations as also a sample corresponding to a healthy meniscus.

All CT images were reviewed and the anatomical structure of interest was manually annotated within the 3D Slicer software for each CT image series. An example of annotated meniscus can be seen in Fig. 2. The corresponding annotations were used to create a 3D representation of the marked area as a surface model for every meniscus model as can be seen in Fig.1. These models are treated as the pre-operative *ground-truth* data.

Since the anatomical structure of interest during the MIS procedure will most probably be occluded during the registration the need of registering small parts of the pre-operative model to the field of view was created. The framework we created can segment the 3D model in smaller areas, extracting small parts of the surface and keeping information regarding the initial model and the area where the segment was extracted. Using this knowledge, we can extract information regarding the success of the registration by measuring the distance of the initial vertices of the *ground truth* model and the corresponding ones in the surface part that is being registered.

In order to create an appropriate dataset[1], we used the mesh model of a healthy meniscus, extracted through manual annotation of the meniscus anatomy on every slice inside 3D Slicer software. Using 25 unique random points on the model as seeds for the segmentation, 50 segmented regions were extracted that had from 15% to 50% of overlapping between them. For every seed we used two different values ($15mm$ and $25mm$) as radius, to determine the size of the segmented patch. Every patch was stored both in point-set and surface form. As an extra feature, noise was added to the models in order to simulate noisy input data from the On-the-fly 3D reconstruction of the surgical field. As an initial step for noise simulation we used a *trivariate Gaussian distribution* ($\mu = 0$, $\sigma = 0.6$). Where 1σ distance ($0.6mm$) in each dimension, corresponds roughly to a total of about $1mm$ error distance. The average *Root Mean Square (RMS)* error between the points of the produced noisy models and the points of initial ones is $1.56mm$. A sample of the segmentation result including added noise can be seen in Fig.3. For each segmented area a point-set and a mesh file are created as well as a corresponding file containing the IDs of the vertices from the initial model that are included in the segment, so all the aforementioned methods (for point-set and surface registration methods) could be evaluated on the same baseline data.

[1]The dataset will be made publicly available and the web link will be added in this footnote upon acceptance of this work

B. Comperative Evaluation Results

Using the aforementioned dataset all methods described here were evaluated on the same base. Both point-based and surface-based methods achieved good registration accuracy in some cases, whereas they failed at some others. We used *RMS* error as a metric to define the correctness of a registration. Since we have *ground truth* information for all patches in our dataset, we can measure the root mean squared distance of all points/vertices in the template patch to the corresponding ones of the target surface/point-set. We determined a value of $RMSerror < 2mm$ to be our threshold for considering a registration as successful. Besides the noise level, and the actual size of the segmented region, the initial position of

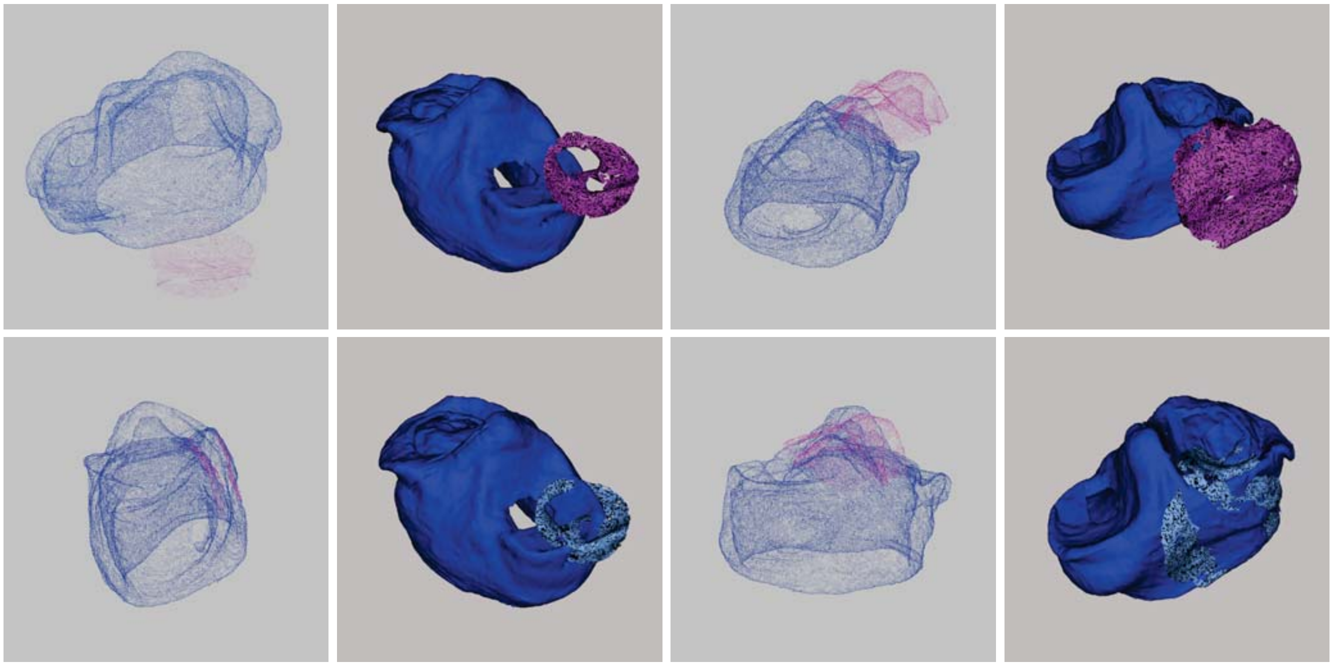

Fig. 6: Examples of erroneous registration results. The initial positions of the template with respect to the target are shown on the top row. The corresponding unsuccessful registration results with convergence $score > 2mm$ are shown on the bottom row (from left to right: ICP, optimal step non-rigid ICP, CPD, diffeomorphic non-rigid).

the template point-set/surface with respect to the target was also parametrized to simulate various initialization errors. The segmented patch was translated and rotated at random distance and orientation in all three axes in every iteration, A detailed evaluation of each approach follows.

1) ICP: This basic approach managed to achieve acceptable registration results in most of the cases to an average convergence error (RMS distance) of $1.92mm$. Through all the examined patches of the dataset, ICP achieved a successful registration in 67.3% of the cases. Although the registration was successful in the majority of the cases, the time needed for converging was one of the highest amongst all, since the average converging time was $2.28sec$. The cases where this approach didn't achieve acceptable results were due to a large initial distance between the two point-sets, thus leading to local minima after a few initial iterations. Despite that, ICP managed to achieve an acceptable registration even when the template patch had a distance of $24mm$ from the target.

2) Optimal Step Non-Rigid ICP: This ICP variant for surfaces achieved similar results with the simple ICP algorithm achieving an overall success rate of 72.6%. The time needed for registration was again too high reaching an average of $2.53sec$ to complete the registration. The average convergence error was $1.84mm$. The registration was successful in the majority of the cases, even in those including a high rate of noise. The cases where this approach didn't achieve acceptable results were again due to large initial distance between the two point-sets, but this method was more sensitive to the initial distance between the template patch and the target one, since the maximum distance between the two patches, that this method achieved a successful registration ($RMS < 2mm$) was $13mm$.

3) Coherent Point Drift: This approach managed to achieve the best registration results with an average convergence error of $1.76mm$ and an overall success rate of 78.8%. Although the registration wasn't successful in all of the cases, it managed to achieve the lowest registration error amongst all examined methods. The cases where this approach didn't achieve a good result were actually again due to a large initial distance between the two point-sets, by achieving acceptable registration with a maximum average distance of $18mm$ between the two point sets. The average time for registration was $1.57sec$, which is not yet acceptable for a real-time framework but the method can be further parametrized trying to reach real-time registration times.

4) Diffeomorphic non-rigid registration of shapes: This approach achieved the lowest acceptable registration success rate of 49.8%, with an average convergence error of $2.63mm$. The time needed for registration was even higher than the ICP reaching an average of $2.74sec$ for converging. The average time needed for convergence was near ICP time, reaching $2.74sec$. The initial distance between the two surfaces didn't seem to cause any drawback in the registration process since the maximum distance for which this method achieved an acceptable registration reached up to $41mm$.

C. Overall evaluation results

It is clear by the above analysis summarised in Table I that a good initialization step is critical for all examined methods. Samples of successful registration can be seen for every examined method in Fig.5, whereas examples of erroneous

TABLE I: OVERALL EVALUATION RESULTS FOR THE 3D REGISTRATION METHODS.

	Success Rate %	**Average convergenceerror (RMS)**	**Maximum initialdistance**	**Average RegistrationTime**
ICP	67.3%	1.92mm	24 mm	2.28 sec
Optimal Step Non-Rigid ICP	72.6%	1.84mm	13 mm	2.53 sec
CPD (non-rigid case)	**78.8%**	**1.76mm**	18 mm	**1.57 sec**
Diffeomorphic	49.8%	2.63mm	**41 mm**	2.74 sec

registrations can be seen in Fig.6. In the majority of the cases where the registration produced large registration errors the initial position of the template with respect to the target was larger than the ones resulting in successful registration. Regarding this attribute, the Diffeomorphic approach presented the best results achieving a successful registration at a maximum initial distance of 41mm. However, with respect to other evaluation metrics, CPD is the method of choice since it achieved on average the lowest RMS error, the highest success rate, and the lowest execution time. The produced results, although promising, indicate the need to research further in the parametrization of the methods in order to improve them. Another critical point we should investigate further is the optimization of the registration process with respect of execution time since the final objective of this framework is to collaborate in real time with On-the-fly 3D reconstruction of the surgical field. Moreover, during this preliminary study, only small deformations of the template surface/point-set were examined. It is crucial to examine larger deformation since the organ surface during the surgical process will undergo large deformations due to interaction with the surgical instruments.

IV. Conclusion

This study describes the comparative analysis of the performance of state-of-the-art 3D registration methods when applied on MIS pre-operative data and simulated intra-operative data. The main motivation for not using actual MIS data is the difficulty of establishing ground-truth correspondences for evaluation of the methods. Instead, we adopted a methodology for deriving surface patches from the pre-operative models and introduce noise into their structures. During this study, we focused the evaluation in rigid transformations, and there is a possibility that this is the reason the point-set to point-set methods outperformed the surface to surface ones. An interesting conclusion is that, as indicated by the results, non-rigid methods can achieve superior performance even for this type of transformation. In the future, we aim to add non-rigid samples in the *ground truth* dataset, containing a scale of small to large deformations, examining whether in those cases the surface to surface registration methods will be more dominant.

As a result of applying the evaluated methodologies to our *ground truth* dataset, we have identified the main problems encountered in MIS registration and broke them down into steps for future examination. Another important note we have extracted from this comparative study is the need to modify these methods for performing in real time. As a next step, we are planning to create a larger dataset, which will include models from different meniscus types, but also different types of organs, in order to be able to evaluate the examined methods in a more complete aspect. In this extended dataset, we intend to add different types and amounts of noise and address large deformations.

Acknowledgment

The authors would like to thank TheMIS Orthopaedic Center of Thessaloniki, Greece, for providing the knee phantom and the corresponding CT image data of the meniscus, that were used for creating the presented dataset.

References

[1] Simpfendrfer, Tobias, et al. "Augmented reality visualization during laparoscopic radical prostatectomy." Journal of endourology 25.12 (2011): 1841-1845.

[2] Figl, Michael, et al. "Image guidance for robotic minimally invasive coronary artery bypass." Computerized Medical Imaging and Graphics 34.1 (2010): 61-68.

[3] Su, Li-Ming, et al. "Augmented reality during robot-assisted laparoscopic partial nephrectomy: toward real-time 3D-CT to stereoscopic video registration." Urology 73.4 (2009): 896-900.

[4] Zeng, Wei, and Xianfeng David Gu. "Registration for 3D surfaces with large deformations using quasi-conformal curvature flow." Computer Vision and Pattern Recognition (CVPR), 2011 IEEE Conference on. IEEE, 2011.

[5] Pessaux, Patrick, et al. "Robotic duodenopancreatectomy assisted with augmented reality and real-time fluorescence guidance." Surgical endoscopy 28.8 (2014): 2493-2498.

[6] Oktay, Ozan, et al. "Biomechanically driven registration of pre-to intra-operative 3D images for laparoscopic surgery." International Conference on Medical Image Computing and Computer-Assisted Intervention. Springer, Berlin, Heidelberg, 2013.

[7] Arun, K. Somani, Thomas S. Huang, and Steven D. Blostein. "Least-squares fitting of two 3-D point sets." IEEE Transactions on pattern analysis and machine intelligence 5 (1987): 698-700.

[8] Besl, Paul J., and Neil D. McKay. "Method for registration of 3-D shapes." Sensor Fusion IV: Control Paradigms and Data Structures. Vol. 1611. International Society for Optics and Photonics, 1992.

[9] Amberg, Brian, Sami Romdhani, and Thomas Vetter. "Optimal step nonrigid ICP algorithms for surface registration." Computer Vision and Pattern Recognition, 2007. CVPR'07. IEEE Conference on. IEEE, 2007.

[10] Myronenko, Andriy, and Xubo Song. "Point set registration: Coherent point drift." IEEE transactions on pattern analysis and machine intelligence 32.12 (2010): 2262-2275.

[11] Luo, Bin, and Edwin R. Hancock. "Iterative procrustes alignment with the em algorithm." Image and Vision Computing 20.5-6 (2002): 377-396.

[12] Guo, Hongyu, et al. "Non-rigid registration of shapes via diffeomorphic point matching." Biomedical Imaging: Nano to Macro, 2004. IEEE International Symposium on. IEEE, 2004.

[13] 3D Slicer, an open source software platform for medical image informatics, image processing, and three-dimensional visualization. [https://www.slicer.org/]